

Model Theory for Scanning Tunneling Microscopy: Application to Au(110)(1×2)

N. García, C. Ocal, and F. Flores

División de Física, Universidad Autónoma, Madrid 34, Spain

(Received 25 April 1983)

A theory is presented for the scanning vacuum-tunneling microscopy experiments performed by Binnig *et al.* The tunnel current is obtained for different geometries and tip shapes. Lateral resolutions are 4–8 Å for distances from the tip to the sample ~ 3.5 –4.5 Å, effective tip radii ~ 3 –10 Å, 1-nA currents, and applied voltage ~ 0.01 eV. The Au(110)(1×2) surface is analyzed and the experimental results discussed.

PACS numbers: 68.20.+t, 73.40.Gk

Recently Binnig, Rohrer, Gerber, and Weibel¹ (BRGW) have been able to control and perform vacuum tunneling of electrons from a W tip to a sample surface. By moving the tip parallel to the surface, they have mapped the Si(111)(7×7) as well as the Au(110)(1×2) and (1×3) reconstructed surfaces.¹ Without doubt, this new technique (scanning tunneling microscopy) opens great expectations in surface physics. The experiments are performed by maintaining constant current, ~ 1 nA, and applying a constant voltage, $V_0 \sim 0.01$ eV, between the tip and the sample. When the tip moves along the surface, it shifts upwards and downwards, giving a description of the surface geometry. In order to interpret all this information, a theory is needed from which to obtain, for instance, the real corrugation charge from the tip motion. This theory must tell us at the same time what are the lateral resolution of a given tip and the current I for a given distance d from the tip to the surface. In this paper we present a

realistic model which gives an answer to those questions and which is applied to Au(110)(1×2).

Our model is graphically described in Fig. 1. The left-hand side is a scheme for the one-electron potential profile between the tip and the sample. There are three important contributions to that potential: (i) First, we have a narrow region of width around 1 Å near the two metals,² where the potential changes quickly from the bulk to the vacuum. (ii) On the other hand, an electrostatic potential between the two metals must be included to equalize both Fermi levels; for W and Au, the voltage drop is 0.7 eV, i.e., the difference in work functions between the tip and the sample.³ (iii) Finally, there must appear corrections introduced by the image potential. Although this effect is important, the image potential is very flat in the region between both metals, presenting important variations only near both surfaces.

According to this discussion, in our model we

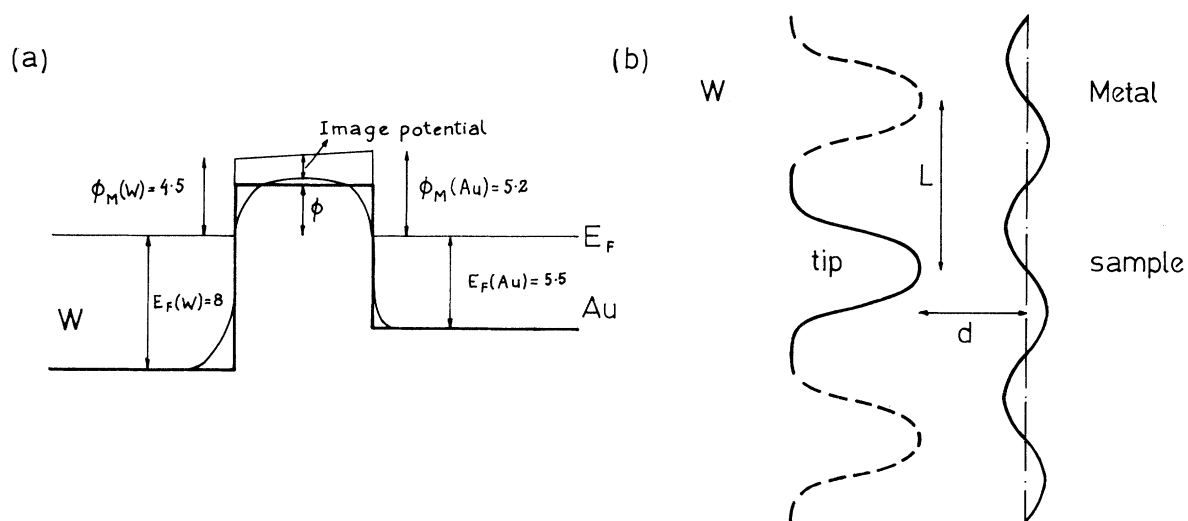


FIG. 1. (a) Energetic scheme of the tip-sample system. (b) Lateral profile of the tip repeated periodically with a period L large enough to decouple the tips.

simplify the interface potential and substitute the abrupt potential shown in Fig. 1(a). We have chosen the parameters of this model in order to simulate the tunneling associated with the s wave functions of both metals,⁴ which are the ones giving the important contribution to the tip current. The following values of the Fermi energies of both media have been used: $E_F(\text{Au}) \approx 5.5$ eV and $E_F(\text{W}) \approx 8$ eV (Ref. 5) (see Fig. 1). In Fig. 1(b), we also show the scheme used in real space for the shape and potential of both surfaces.

Having defined the model, our problem is to solve for the current density, the transmissivity, and the reflectivity of one electron approaching the tip's surface from $+\infty$ and tunneling to the sample. The total intensity is obtained from all the electrons contained in a spherical shell around the tip's Fermi surface with an energy width equal to V_0 , which in the experiments¹ is taken as around 0.01 eV.

This problem has been solved by periodically repeating the tips across the surface [Fig. 1(b)], at distances L large enough to leave them decoupled. We have used the same numerical techniques as developed in atom⁶ and light surface scattering.^{7,8} We have analyzed different systems with a corrugated surface (either W or Au) having spherical, cosinelike, parabolic, and saw-tooth profiles, placed at a distance d from a plane surface (either Au or W). By using 50 reciprocal-lattice vectors, we have obtained highly convergent results. In our calculations, we have obtained the total intensity I going from the tip to the sample for a given V_0 and d , and energy φ (this is the Fermi energy as measured from the vacuum level, Fig. 1), as well as the maximum current density, j_0 , at the sample surface. From these two quantities I and j_0 , we can define an effective length, L_{eff} , related to the sample surface area (lateral resolution) scanned by the tip:

$$\pi(L_{\text{eff}}/2)^2 = I/j_0. \quad (1)$$

The values of the current density, j , as a function of the distance from the center of the tip are presented in Fig. 2 for $R_{\text{eff}} = 10 \text{ \AA}$ [cf. Eq. (3) below] and $d = 3.5 \text{ \AA}$. Notice the rainbow effect as the incident angle, θ_i , of the electrons increases. The intensity is the summation of the integrals of the continuous curves given in Fig. 2. It should be commented that the typical transmissivities for $d \approx 3.5\text{--}5 \text{ \AA}$ are $\sim 10^{-2}\text{--}10^{-3}$.

A very interesting result connected with our intensity calculations is that I can be written in

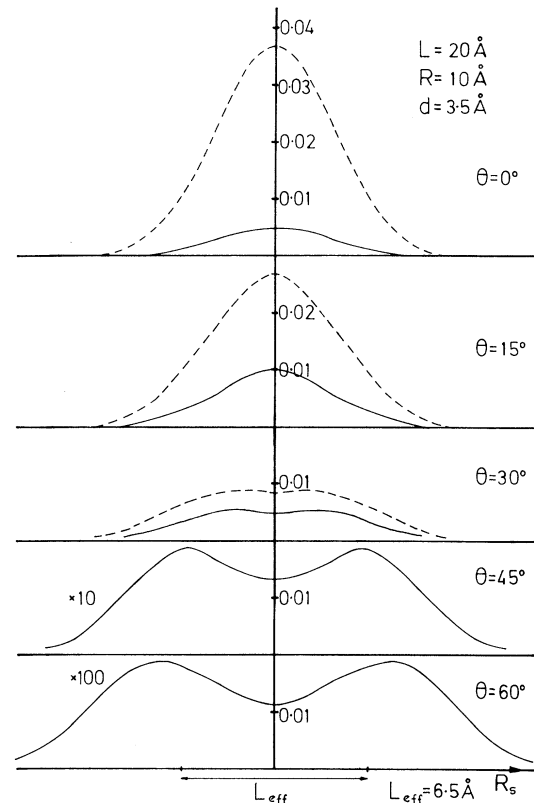


FIG. 2. Current density j for a spherical profile, as a function of the distance to the center of the tip. It has cylindrical symmetry. Dashed lines are the currents of one electron at a given incident angle θ_i . The continuous curves are the dashed lines multiplied by the averaged solid angle of the Fermi sphere. The radius of the tip is 10 \AA , $L = 20 \text{ \AA}$, $\varphi = 4.5$ eV, and $d = 3.5 \text{ \AA}$.

the following way:

$$I = \frac{e\hbar}{2m} G N(E_F) V_0 \exp \left[-2.14 \left(\frac{2m\varphi}{\hbar^2} \right)^{1/2} d \right], \quad (2)$$

where $N(E_F)$ is the density of states at the Fermi level for the tip, and G is a constant depending only on the geometry of the sample and the tip, and is related to the transmissivity from W to Au. Furthermore, we have found that G is practically only a function of an effective curvature, R_{eff} , defined as follows:

$$\frac{1}{R_{\text{eff}}^2} = \left(\frac{1}{R_1^t} + \frac{1}{R_1^s} \right) \left(\frac{1}{R_2^t} + \frac{1}{R_2^s} \right), \quad (3)$$

where $R_{1,2}^t$ and $R_{1,2}^s$ are the two radii of curvature associated with the tip and the sample, respectively. Figure 3(a) shows the dependence of G on R_{eff} .

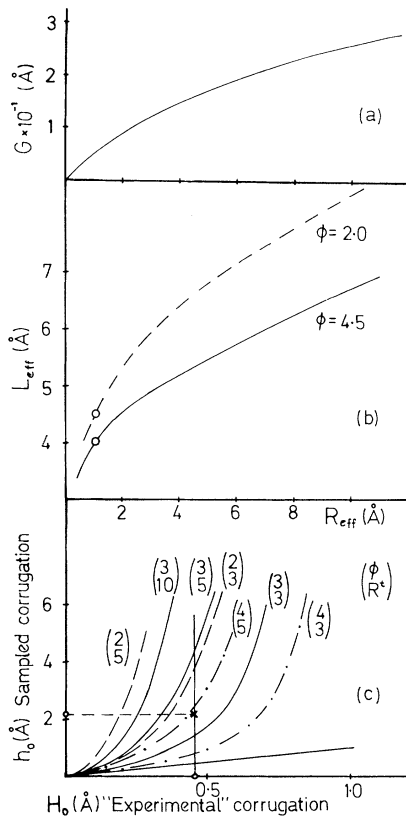


FIG. 3. (a) Values of G vs the effective radius of curvature of the tip-sample system, R_{eff} [formula (3)]. (b) L_{eff} for the same values of R_{eff} . The system W-Au is indicated by the circles with 4–4.5 \AA resolution. (c) Values of the experimentally observed corrugation H_0 as a function of the sampled corrugation h_0 . The curves are given for $(\phi$ (eV); R^t (\AA)). For Au(110)(1 \times 2), $H_0 \approx 0.45$ \AA , $\phi = 3$ eV, $R^t \approx 3.5$ \AA , $h_0 \approx 2.1$ \AA , and $d \approx 4$ \AA . This is indicated by the cross.

Returning to Eq. (2), it is of interest to comment that the exponent that we have found, $\exp[-2.14(2m\phi/\hbar^2)^{1/2}d]$, is quite close to the one that appears for plane surfaces,⁹ $\exp[-2 \times (2m\phi/\hbar^2)^{1/2}d]$, for the current density. We argue that the small difference that we have found in the exponent, 2.14 compared to 2, is due to the curvature of the two surfaces; note that this curvature increases the effective distance between the two metals. On the other hand, note that our results have been found for $R_{\text{eff}} \lesssim 11$ \AA .

In Fig. 3(b) we give L_{eff} , as defined by Eq. (1), as a function of ϕ and R_{eff} for $I = 1$ nA and $V_0 = 0.01$ eV (the dependence on d is small and has not been included in this figure). The values found for L_{eff} are between 4 and 8 \AA . Then, we

have analyzed the corrugation H_0 observed¹ by the tip in its motion (~ 0.45 \AA) as a function of the cosinelike roughness, $\frac{1}{2}h_0 \cos[(2\pi/a)x]$, assumed to appear on the Au(110)(1 \times 2) surface,^{1,4} a being the unit-cell length. The maximum and minimum of the tip position have been analyzed by using Eq. (2), for $V_0 = 0.01$ eV, $I = 1$ nA, and $N(E_F) = 2 \times 10^{22}$ cm³/eV; from this equation we obtain d , ~ 3.9 \AA , and determine the tip position. Note that in the minimum position, the tip "touches" the sample at two points, in such a way that through each one we have an intensity of ~ 0.5 nA.

In Fig. 3(c) we give the dependence of H_0 on h_0 , for different values of ϕ (2, 3, and 4 eV) and the tip radius, R^t . Our results show how H_0 tends to saturate for high h_0 values, a quite obvious result. Figure 3(c) also shows that in order to get very high resolution we need very small tip radii. However, for R between 3 and 5 \AA , we have quite a reasonable resolution. Referring to the BRGW results for Au, it is of interest to comment on the value of H_0 , ~ 0.45 \AA , as found¹ for the (1 \times 2) surface. The same surface has been analyzed by atom scattering,⁴ and a roughness of $h_0 = 1.4$ \AA was found, when the turning point of the incident atoms is ~ 3.5 \AA from the surface; this is a low limit to the roughness of the surface potential, as shown in Fig. 1. Taking into account this result and Fig. 3(c), we conclude that the effective radius of the tip used by BRGW for Au must be 3.5 ± 0.5 \AA and the distance from the maximum $d_{\text{max}} \approx 3.9$ \AA .

We should comment that we expect ϕ to be around ~ 3 eV, a value which is obtained by assuming that the image potential lowers the barrier by ~ 1.7 eV. At this point it is worth commenting that Eq. (2) can be used to calibrate the effective value of ϕ in the experiments. To this end, the intensity I should be drawn as a function of d in a semilogarithmic scale. Although in principle ϕ is a function of d (as a result of image potential effects), that plot must show essentially a linear relationship between I and d for small changes of d . Moreover, for large variations of d , Eq. (2) could be used to analyze the image potential.

We believe that the results presented here have general characteristics, and that the effects associated with nonabrupt potentials can be introduced by an effective value of ϕ .

We thank A. Baratoff for discussions and H. Rohrer and G. Binnig for comments on their experiments.

¹G. Binning, H. Rohrer, Ch. Gerber, and E. Weibel, *Appl. Phys. Lett.* **40**, 178 (1982), and *Phys. Rev. Lett.* **49**, 57 (1982), and **50**, 120 (1983), and recent results for Au(110)(1×2).

²N. D. Lang and W. Kohn, *Phys. Rev. B* **1**, 4555 (1970); N. D. Lang, in *Solid State Physics: Advances in Research and Applications*, edited by H. Ehrenreich, Frederick Seitz, and David Turnbull (Academic, New York, 1973), Vol. 28, p. 225.

³J. Hölz and F. K. Schulte, in *Solid Surface Physics*, Springer Tracts in Modern Physics Vol. 85 (Springer, Berlin, 1979), p. 98, Table 4.3.

⁴N. García, J. A. Barker, and I. P. Batra, *J. Elec-*

tron Spectrosc. Relat. Phenom. **30**, 137 (1983).

⁵C. Kittel, *Introduction to Solid State Physics* (Wiley, New York, 1971), 4th ed., p. 248, Table 1.

⁶N. García, *J. Chem. Phys.* **67**, 897 (1977); N. García and N. Cabrera, *Phys. Rev. B* **18**, 576 (1978).

⁷N. García, to be published; N. E. Glass, A. A. Maradudin, and V. Celli, *Phys. Rev. B* **27**, 5150 (1983).

⁸It should be stated that convergent results are obtained for this problem as well as for light scattering for a much larger corrugation than for hard walls in atom-surface scattering.

⁹C. B. Duke, *Tunneling in Solids*, Solid State Physics Suppl. 10 (Academic, New York, 1969).